Reassigned Short Time Fourier Transform and K-means Method for Diagnosis of Broken Rotor Bar Detection in VSD-fed Induction Motors

Noe Alejandro OJEDA-AGUIRRE[1], Arturo GARCIA-PEREZ[1],
Rene de Jesus ROMERO-TRONCOSO[2], Daniel MORINIGO-SOTELO[3],
Oscar DUQUE-PEREZ[3], David CAMARENA-MARTINEZ[1*]

[1]*CA Digital Signal Processing, Engineering Divison, Campus Irapuato-Salamanca, University of Guanajuato, 36700 Salamanca, México*
[2]*CA Mecatronics, School of Engineering, Autonomous University of Queretaro, Campus San Juan del Rio Moctezuma 249, 76807 San Juan del Rio, Qro., Mexico*
[3]*Department of Electrical Engineering, University of Valladolid (UVa), 47011 Valladolid, Spain*
dcamarena@hspdigital.org

Abstract—**Over the years induction motors have established an uncanny knack for providing a plethora of utilities in the industry, where the fault monitoring and detection has become necessary. Several techniques could be applied for the monitoring and identification of broken rotor bars when the motor is fed by a variable speed drive (VSD). Nevertheless, many of these methodologies detect this fault and other failures in the steady state condition, but this monitoring grow into more complicated analysis during the startup transient condition owing to the large number of harmonics, which the VSD insert to the current signal. The novelty of the proposed methodology is the application of the reassignment during the startup transient and the steady state conditions to identify one broken rotor bar in the induction motor. The proposed methodology is experimented with both, real and synthetic signals. The problems that Short Time Fourier Transform (STFT), shows for the identification of broken rotor bars are exhibited. The proposed methodology includes an automatic diagnosis (K-means algorithm), where the signal energy is used. The results show that the Reassigned Short Time Fourier Transform (RSTFT) technique and K-means methods are appropriated for the effective monitoring and diagnosis of one broken rotor bar in the induction motor during the startup and steady state conditions of operation.**

Index Terms—**induction motors, fault diagnosis, rotors, digital signal processing, spectral analysis.**

I. INTRODUCTION

Induction motors (IM) have established an uncanny knack for providing a plethora of utilities in the industry; however, they are susceptible to internal faults such as broken rotor bar (BRB), and this fault is one of the commonly found in the IM that may cause serious motor harm if this fault is not detected timely. The IM are exposed to different mechanical, magnetic, electrical, and thermal stimulus, which frequently could cause failures [1]. From all possible failures, the BRB is one of the most difficult faults to identify, since the motor seems to be working supposedly in a normal way; but this fault could produce several other problems to the mechanical systems coupled to it.

In recent years, considerable research and efforts have been made on the study and development of methodologies used for monitoring and early fault diagnosis, being the Condition-Based Maintenance (CBM) one of the techniques with considerable success by his non-invasive nature. Specifically, for squirrel cage IM, BRB faults account for approximately 10% of all failures [2,3]; therefore, the incipient monitoring and identification of this fault is a big concern.

Several methods and techniques have been used recently for detection of BRB [1], [6-18]; where Motor Current Signature Analysis (MCSA) is one of the most important monitoring techniques by its noninvasive, precise, and easy of use. These characteristics has been widely used to diagnose failures in electrical motors such as broken rotor bar fault, air gap eccentricity, or mass unbalance fault and stator winding fault [5]. Specifically, for BRB fault, MCSA is simply the process by which motor current signals are recorded and analyzed in the frequency domain [4, 5]. In this sense, a great number of investigations use several techniques namely, Fast Fourier Transform (FFT), Discrete Wavelet Transform (DWT), Empirical Mode Decomposition (EMD), and some others for MCSA analysis of IM. A great number of researches concentrate on the line fed IM analysis; where several approximations can be found, which make the MCSA useful in steady state, startup transient, or both conditions for the monitoring and diagnosis of BRB's. For example, the authors of [6] use Mathematical Morphology (MM) programmed to use VHDL (Very High-Speed Integrated Circuits Hardware Description Language) on a FPGA for real-time online applications to identify one and two BRB´s in steady state with also different load levels. In [7], authors use a combination of a filter bank and the Multiple Signal Classification (MUSIC) algorithm to detect multiple combined faults by analyzing the vibration and the steady state current signals. In [8], authors detect rotor faults with the use of both, the maximum covariance method and zoom FFT (ZFFT), for frequency tracking of the stator current at steady state. The use of EMD to extract fault related patterns from the original startup current signals by applying the Hilbert–Huang Transform (HHT) and the Scale transform

(ST), for invariant feature selection and automatic diagnostic of the condition of the electric machine, is proposed in [9]. In [10], authors detect BRB's in startup transient, in steady state condition with various load levels using the MCSA of intrinsic mode functions, as well as using the EMD technique. VSD-fed IM is the most common use of IM in industry applications; for example, in [11], authors present the MUSIC technique for a VSD-Fed IM during the startup transient by analyzing the MCSA of a healthy motor and an IM with one BRB in different levels of load, in order to quantify the evolution of the fault, and the rms value, and characteristic values are obtained for each case. In [12], a smart sensor is presented for online monitoring; where one or multiple combined failures in IM fed through a VSD in a wide frequency range from 3 Hz up to 60 Hz; with the use of FFT and combined with Artificial Neural Networks (ANN) during steady state condition. In [13], the current spectrum analysis is presented at steady state for feeding the line with two different drives under three levels of load and three different frequencies of the VSD; for incipient detection of broken rotor bars by using a combination of the spectral techniques such as FFT, Wavelet+FFT, MUSIC, EMD+FFT, EMD+MUSIC, where effectiveness is evaluated for each methodology. In [14], a study for the detection of inter-turn faults on IM fed inverter, during the start-up transient and steady-state with the use of the FFT, the discrete wavelet transform (DWT), and Wavelet Packets Decomposition (WPD), is presented. The authors of [15,16] propose the Chirplet Transform (CT), and the Adaptive Slope Transform (AST) in a VSD-fed IM in the startup transient to detect the fault related harmonics evolution and the eccentricity related harmonics. The authors in [17] performed a statistical analysis for classification of different sets of failures in IM inverter fed, using an artificial neural network, and the implementation is done in FPGA to offer an online solution on a single chip (SoC), for real-time monitoring. In [18] authors perform an analysis of Intrinsic Mode Functions (IMF) obtained by EMD for one or multiple broken bars and different load levels and operating speeds, for line start and inverted fed IM. Thus, to secure the proper IM functionality is necessary to monitor and detect faults in the startup transient, as well as in the steady state conditions. However, in recent works, it has been observed that the startup transient needs to be further studied, since the type of transient depends largely on the control strategy; where different patterns of the fault can be extracted [1]. On the other hand, when the IM is fed inverted, extra harmonic content is added in the stator current, developing small values of rotor slip, which make those spectral components fault-related to evolve closely to the fundamental frequency during startup transient condition, and making the fault difficult to detect [11, 21].

Other useful analysis tools applied in fault diagnosis are the classification techniques [23]. Recently, different classification methods such as fuzzy logic [24-27] and neural networks [28-31] have been applied to monitoring and diagnose the condition of IM. However, some artificial intelligent techniques have limitations on generalization of conditions when the number of samples is limited [32]. Therefore, with the need of a simple diagnosis technique, a small number of samples, and good efficiency; it is

proposed the K-means algorithm for this purpose, which has been proved with good results [33, 34].

In this paper, the reassigned Short Time Fourier Transform (RSTFT) is applied to the current signal of a VSD-fed IM in both, the startup transient/steady state conditions, to identify the sideband components related to the failure of BRB in the IM: Lower Sideband Harmonic (LSH) and Upper Sideband Harmonic (USH). The analysis is validated by identifying the conditions of IM, using the K-means algorithm for one broken rotor bar, and the healthy conditions during the startup transient/steady state at different VSD-fed frequencies, and the obtained results shows the effectiveness to the proposal.

II. THEORETICAL BACKGROUND

A. Short-Time Fourier Transform (STFT)

Short-Time Fourier Transform is a technique derived from the Fourier transform in time-frequency (1), for a function $x(t)$, using a window $h(t)$, and it is defined as:

$$STFT_x^h(t,f) = \int_{-\infty}^{\infty} x(t') h^*(t'-t) e^{-j2\pi ft'} dt' \quad (1)$$

Where x is a function of time t, then Short-Time Fourier Transform $STFT_x^h$ is a function of time t and frequency f. It is observed that the transformation $x \rightarrow STFT_x^h$ is linear and it depends on the chosen window $h(t)$. The window $h(t)$ is generally an even function and it is concentrated around time and frequency zero respectively, where the function and its FT are maximal.

The time and angular frequency have a symmetric role, and another representation of *STFT* can be made [20]:

$$F_x^g(t,\omega) = \int_{-\infty}^{\infty} x(s) g^*(s-t) e^{-j\omega s} ds \cdot e^{j\omega t/2} \quad (2)$$

In the STFT, that constraint of study around the moment t will be gotten using a discretionary window $g(t)$. This second definition contrasts from the first one by the exponential factor $e^{j\omega t/2}$, and by using precise angular frequency ω, rather than frequency f; where time and angular frequency assume a symmetric role. The STFT has a struggle between a good resolution in time or frequency, since a narrow window $g(t)$ will provide a good time resolution, but a poor frequency resolution. On the other hand, when a long analysis window is chosen, the obtained spectrum provides a poor time resolution and good frequency resolution.

B. The Reassignment principle

Given an STFT F_x^g, the spectrogram S_x^g is defined as:

$$S_x^g(t,\omega) = \left| F_x^g(t,\omega) \right|^2 \quad (3)$$

But this can be written in the following form:

$$S_x^g(t,\omega) = \int_{-\infty}^{\infty}\int_{-\infty}^{\infty} \frac{W_x(s,\eta)}{W_g(s-t,\eta-\omega)^{-1}} \frac{dsd\eta}{2\pi} \quad (4)$$

This, unequivocally, demonstrates that the used window provides a smoothing spectrum over-time and frequency domains of the Wigner-Ville Distribution (WVD). This

transformation represents an energy density, which is obtained by making the correlation of the signal and a translated version of the same signal. Consequently, the value taken for the spectrogram at a given point (t, ω) cannot be considered as pointwise. In other words, an entire distribution of values is encapsulated to a unique number, which might be, thereby, assigned to the middle point, from a geometrical point of view, in the region where the distribution is considered. In this sense, if the distribution of the total mass of an object is oriented to its geometrical center; with the exception, of a uniform distribution, a more significant choice is made by assigning to the center of gravity of the distribution, the total mass. Therefore, the reassignment principle consists, precisely, of the time-frequency plane at each point (t, ω), where the evaluation is carried on the spectrogram. Then, $\hat{t}$ and $\hat{\omega}$, two additional quantities, are calculated. The local centroids W_x obtained by WVD are multiplied by the time-frequency window W_g in, which it is centered at c; then, the value of the spectrogram calculated at (t, ω) can be determined by:

$$\hat{t}_x(t,\omega) = \frac{1}{S_x^g(t,\omega)} \int_{-\infty}^{\infty} \int_{-\infty}^{\infty} \frac{sW_x(s,\eta)}{(W_g(s-t,\eta-\omega))^{-1}} \frac{dsd\eta}{2\pi} \quad (5)$$

$$\hat{\omega}_x(t,\omega) = \frac{1}{S_x^g(t,\omega)} \int_{-\infty}^{\infty} \int_{-\infty}^{\infty} \frac{\eta W_x(s,\eta)}{(W_g(s-t,\eta-\omega))^{-1}} \frac{dsd\eta}{2\pi} \quad (6)$$

The reassigned spectrogram is, thus, defined by:

$$\hat{S}_x^g(t,\omega) = \int_{-\infty}^{\infty} \int_{-\infty}^{\infty} \frac{S_x^g(s,\eta)}{\delta\left(t - \hat{t}_x(s,\eta), \omega - \hat{\omega}_x(s,\eta)\right)^{-1}} dsd\eta \quad (7)$$

Where $\delta(x,y)$ is the two-dimensional Dirac impulse, for which:

$$\int_{-\infty}^{\infty} \int_{-\infty}^{\infty} f(x,y) \delta(x-x_0, y-y_0) dxdy = f(x_0, y_0) \quad (8)$$

For any function f belonging to $L^2(\mathbb{R}^2)$

STFT can be used to obtain the parameters $\hat{t}$ and $\hat{\omega}$ used in the reassignment. It is important that the phase information obtained by STFT is for the most part not considered when using the spectrogram shown in (3). Considering $\phi(t,\omega)$ such as the STFT phase, and if we use the short notation $\partial_u \phi := \partial\phi / \partial u$, the two reassignment operators can be written as:

$$\hat{t}_x(t,\omega) = \frac{t}{2} - \partial_\omega \phi(t,\omega); \quad (9)$$

$$\hat{\omega}_x(t,\omega) = \frac{\omega}{2} + \partial_t \phi(t,\omega); \quad (10)$$

These variables represent the local instantaneous frequency and the signal group delay being studied, respectively, which initial intention was to uphold the energy concentrations in the neighborhood local instantaneous frequencies and group delays [19].

Conceptually, reassignment is a two-step process:
1. A smoothing operation through a window, which cleans up oscillatory interferences, but its disadvantage is to spread the components;

2. A compression operation, which refocuses the contributions that have survived the smoothing operation [19,20].

Reassignment is a procedure having the objective of building coherent time–frequency representations with efficiency that has been demonstrated, producing a clear time frequency analysis, particularly at high SNR. [19], improving the resolution in order to better visualize the frequency components of the signal.

C. Fault Related Components

The IM with a BRB is distinguish by the existence of sidebands components around the supply current frequency f_m as follows [22]:

$$f_{BRB} = (1 \pm 2s_l) f_m \quad (11)$$

Where f_{BRB} represents the sideband, which are the frequencies associated with the broken rotor bar, and s_l is the per-unit motor slip. The slip s_l is the relative mechanical speed of the motor n_m with respect to the motor synchronous speed n_{sl} as follows:

$$s_l = \frac{n_{s_l} - n_m}{n_{s_l}} \quad (12)$$

The motor synchronous speed n_{s_l} is related to the electrical supply frequency f_m as follows:

$$n_{s_l} = \frac{120 f_m}{p} \quad (13)$$

Where p is the number of motor poles, and the constant "120" is used to express the motor synchronous speed n_{s_l} in revolutions per minute units.

D. K-means

K-means is a simple algorithm to implement and has a good efficiency to cluster a dataset with similar characteristics [33]. This algorithm can be applied to small, medium, or big datasets; and modifying the size of data, affects the processing time to find a solution. It is possible to take a data set of n objects and partition it into k clusters following the next steps: i) select k numbers of objects randomly from dataset to initially represent the centers of k clusters; ii) for each object that is not assigned to a cluster, an object is assigned to any cluster based on the distance toward the center of the cluster; iii) new centers are obtained in order to minimize the objective function, which are defined as [35]:

$$E(m_1,\ldots,m_k) = \sum_{i=1}^{k} \sum_{j=1}^{M_i} \left\| x_{ij} - m_i \right\|^2 \quad (14)$$

Where M_i is the number of objects for each ith cluster, x_{ij} is the jth object of the ith cluster, and m_i is the center of the ith cluster, where $i=1,\ldots, M$ is expressed as:

$$m_i = \frac{1}{M_i} \sum_{j=1}^{M_i} x_{ij}, \quad (15)$$

III. EXPERIMENTAL SETUP

The startup transient and steady-state conditions are studied through the current signal to perform a comparative study that evaluates the effectiveness of the implemented methodology in this research for broken rotor bar detection in a VSD fed IM. Fig 1 indicates the general view of the experimental setup, composed by a tested IM of 1.1 kW three phase induction motor model SIEMENS 1LA7090-51, which is fed with a power supply of a VSD (ACS355) by ABB. The VSD is studied supplying three frequencies at 50 Hz, 65 Hz, and 100 Hz. A mechanical load includes a Lucas–Nülle SE 2662-5R electromagnetic brake with its control unit. In order to acquire the current signal, a proprietary board with Honeywell CSNE151Hall-effect current sensors is used. For data acquisition, National Instruments cDAQ-9174 board with a 16-bit NI 9215 acquisition module, are used.

A sampling frequency of 5 kHz is used by the instrumentation system to collect the three current signals studied at 50 Hz, 65, and 100 Hz. The assays were done of a startup transient continued by a steady state conditions with constant load torques. The VSD-inverter is scheduled to feed a controlled startup where the voltage frequency growth linearly from 0 to 50 Hz, 0 to 65 Hz, and 0 to 100 Hz during 10 s respectively. Tests were accomplished, firstly, with the healthy motor (HLT); next, the same motor with one BRB condition. The BRB was made-up synthetically by drilling a hole of 18 mm into one of the rotor bars in the IM without harming the rotor shaft as is shown in Fig. 2.

Fig. 3 shows the proposed methodology for the BRB identification by using the current signal of one of the IM phases. After the digital-analog system (DAS) stage, a preprocessing module is used to reduce the bandwidth of the signal where the fault-related spectral components are found. A lowpass filter is used to truncate the signal in time domain; then, the RSTFT algorithm is applied for the identification of fault related spectral components. The RSTFT spectrum contains the signal energy distributed over a range of frequencies in the time-frequency domain; where the amplitude of the signal energy e_t, for $t= 0,1,2…16$, in each second during the transient and steady regimes are used as feature input of K-means clustering algorithm, in order to classify them between healthy or faulty conditions (1BRB). The first step in the implementation of K-means algorithm is

to find the initial centroids values; due to it is an unsupervised classification method; a bad selection of the initial cluster values can conduce to wrong clusters selection. In order to afront this problem and to obtain correct initial values of this cluster centers; it is obtained the mean (μ) from a data set of 38 healthy signals and 38 faulty signals of the energy amplitude sampled each second. These values of mean are used as the initial centroids for the clusters representing the faulty and healthy conditions at steady state and startup transient. Then, 100 random values of energy amplitude are generated, bounded by $\mu\pm3\sigma$, where σ is the standard deviation, in order to guarantee an occurrence of 99.7 %, for each second during transient and steady state regimes; then, the final centroids of the clusters by using K-means algorithm are obtained. Finally, a new dataset, of 38 faulty signals and 38 healthy signals is classified in the clusters (healthy and faulty conditions) by using the Euclidean distance of the amplitudes of energy to the centroids of the cluster.
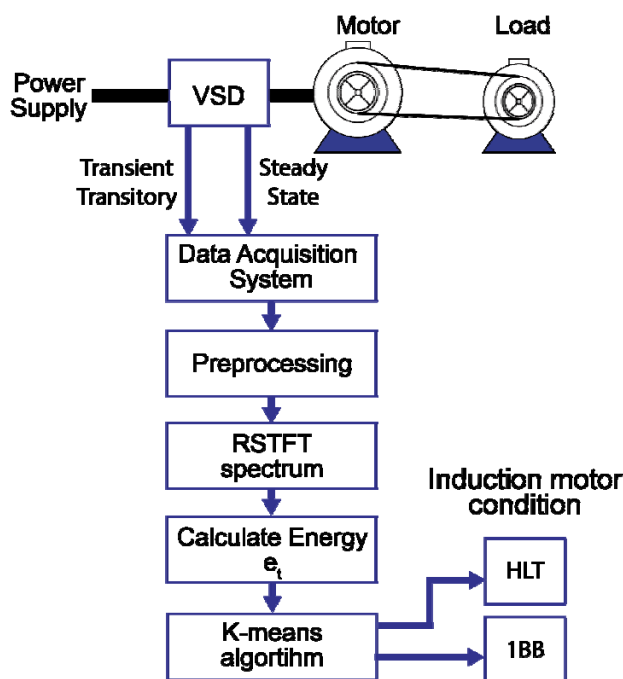

Figure 2. Artificially generated fault.

Figure 1. General view of experimental setup.

Figure 3. Block diagram of the proposed methodology for the VSD fed induction motor.

IV. RESULTS

In order to prove the viability of the RSTFT technique, for broken rotor bar detection, the algorithm is applied to both stator current, and synthetic signals, this last have the typical waveform of startup transient of a VSD fed IM. Initially, the goal is validating the effectiveness of the proposed methodology for synthetic signals with noise and next under real conditions. For comparison purposes, healthy and faulty cases are tested by the STFT and RSTFT using MATLAB software.

Synthetic signals are used to validate new techniques and processes, because their results can be determined previously; since these signals represent a mathematical model of behavior in any physical phenomenon, with the advantage, in comparison with the real signals, of being able to adjust certain parameters important for their study. Fig. 4 shows synthetic signals for a healthy motor VSD-fed IM at 50 Hz and for 1 BRB; synthetic signals are generated considering a 10 second startup transient from 0 a 50 Hz and a steady state from 10 to 20 seconds, which are generated using a linear chirp signal for the startup transient and a 50 Hz tone for the steady state. Furthermore, for faulty motor, the two sideband harmonics, LSH and USH parallel, are considered to the main frequency through startup and steady states, which are generated through two linear chirp signals parallel to main frequency during startup transient, and two tones at 45 and 55 Hz simulating the fault harmonics. For these synthetic signals, a 2.5 kHz sampling frequency is used obtaining 50000 samples, then the signals are decimated to observe the frequency range of interest from 0 to 60 Hz. Additionally, a 0.3 dB Signal-to-Noise ratio level is used in the synthetic signal to test the efficacy of the proposed methodology, even in noise presence.

Fig. 4a shows the time-frequency spectrum of a synthetic signal of a healthy VSD-fed IM, and with Gaussian noise added, where it can be clearly noted that the frequency increases in the startup transient and remains stable at 50 Hz at the steady state by using the STFT technique.

Fig. 4b shows the time-frequency spectrum obtained by the STFT of a synthetic signal for a VSD-fed IM with the broken rotor bar; with two fault-related harmonics, separate 5 Hz from the main frequency of 50 Hz during startup transient and steady state. In the same way, Fig. 4c and Fig. 4d show the time-frequency spectrum of the same synthetic signals, healthy and faulty conditions, but analyzed by the RSTFT technique, where the evolution of the frequency can be noted during startup transient and steady state regimes. However, a higher frequency can be clearly observed, as well as time resolution compared with the STFT. Fig. 4d shows the spectrum of the BRB condition of a VSD-fed IM, where the two fault related harmonics appear, which are separate 5 Hz from the main frequency of 50 Hz during startup transient and steady state; a better time and frequency resolution is shown by using RSTFT in comparison with the STFT.

Fig. 5a shows stator current STFT spectrum for a healthy IM, and Figs. 5b-5d present the spectra for one BRB VSD fed IM at 50 Hz, 65 Hz, and 100 Hz, respectively. A sampling frequency of 5 kHz is used for 10 seconds, obtaining 50000 samples, then the signals are decimated to analyze the respective interest region; where the a priori known frequencies are localized for broken rotor bars failure from 0 to 60 Hz for 50 Hz signal, 0 to 90 Hz for 65 Hz signal and 0 to 120 Hz for 100 Hz signal. Fig. 5a shows the
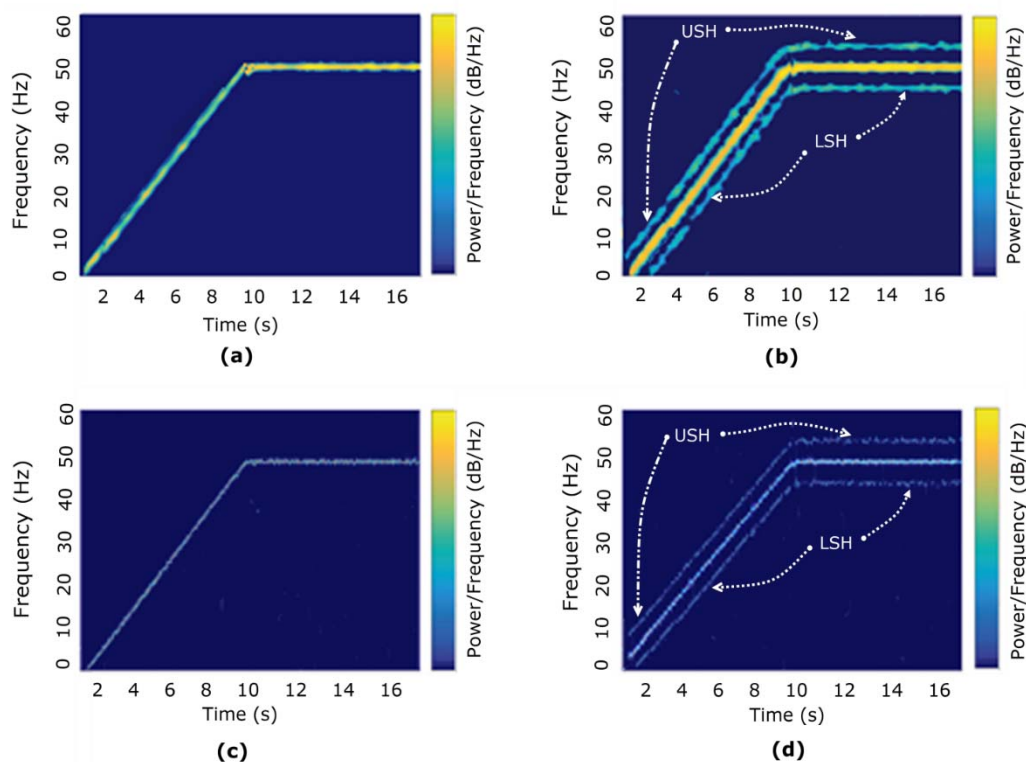

Figure 4. Simulation for synthetic signals: a) Healthy with STFT, b) One broken rotor bar with STFT (Time evolution of rotor frequency and fault related harmonics for BRB (lower sideband harmonic (LSH) and upper sideband harmonic (USH); c) Healthy with RSTFT, and d) One broken rotor bar with RSTFT VSD Fed at 50 Hz, and their fault related harmonics (USH and LSH).
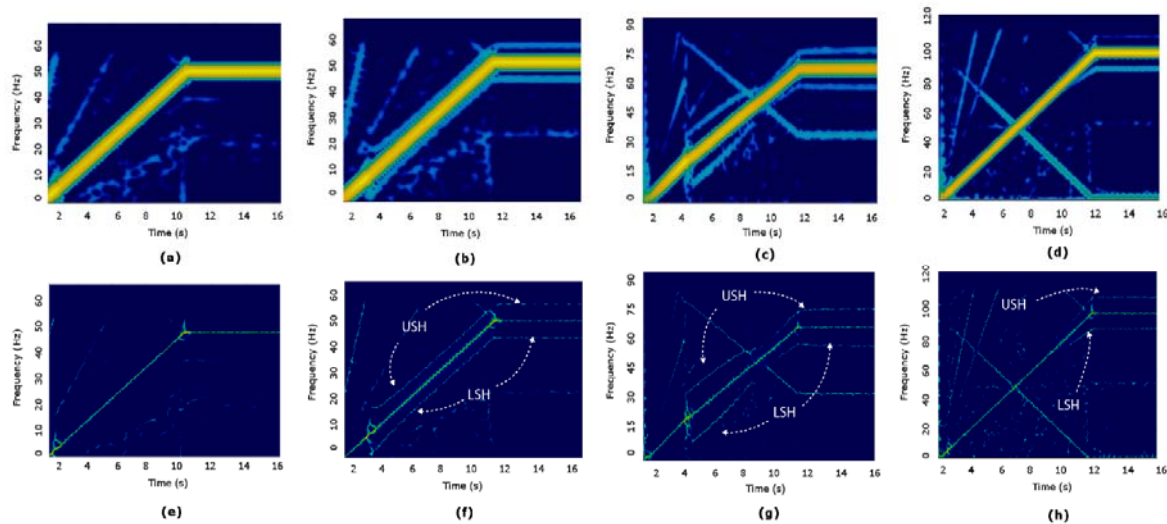
Figure 5. Real signals for a) Healthy with STFT VSD Fed at 50 Hz, b) One broken rotor bar with STFT VSD Fed at 50 Hz, c) One broken rotor bar with STFT VSD Fed at 65 Hz d) One broken rotor bar with STFT VSD Fed at 100 Hz, e) Healthy with RSTFT VSD Fed at 50 Hz, f) One broken rotor bar with RSTFT VSD Fed at 50 Hz, g) One broken rotor bar with RSTFT VSD Fed at 65 Hz and h) One broken rotor bar with RSTFT VSD Fed at 100 Hz

time-frequency spectrum by STFT of the startup transient from 0 at 10 seconds and steady state 10 onwards for a healthy VSD-fed IM, where the fault harmonics related to the BRB does not appear all the time.

Fig. 5b shows the STFT spectrum for BRB condition at 50 Hz, where the fault-related harmonics can be observed during the steady state. However, the evolution of these harmonics is not clearly related to fault (LSH and USH) during startup transient because there is no clear separation from the main frequency at 50 Hz.

Fig 5c shows the STFT spectrum for BRB condition at 65 Hz, where the LSH and USH can be observed during the steady state, regarding to startup transient the fault-related harmonics can be partially observed from 4 to 10 seconds, but in the forward seconds there is no clear separation from main frequency at 65 Hz.

Fig. 5d shows the case for VSD-fed IM at 100 Hz with STFT, where the evolution of main frequency and LSH during steady sate can be observed, and during startup transient, there is no clear separation of LSH from the main frequency.

The time-frequency representation of the stator current signal of a healthy motor is shown in Fig. 5e, where the startup transient goes from 0 to 10 seconds and steady state can be observed, also, where several harmonics around the startup transient, but with a better resolution compared to the classical STFT technique.

Fig. 5f shows the stator current signal spectrogram of the IM during the startup transient, where the evolution of the main frequency during startup transient and steady state can be clearly observed. The evolution of one broken rotor bar related harmonics LSH and USH during these two states using the RSTFT, can be observed as well.

In Fig. 5g, the RSTFT spectrogram is shown for the stator current signal of VSD fed IM at 65 Hz, where a few harmonics induced by the VSD can be observed. The evolution, of fundamental frequency; LSH and USH during startup transient; and steady state using the proposed technique RSTFT, is clear.

Finally, the Fig. 5h shows the image for the stator current signal of VSD fed IM at 100 Hz, with one BRB during startup transient and steady state, where it can be observed the main frequency evolution and LSH evolution during the last two seconds approximately of the startup transient and during the steady state with the use of RSTFT.

Table I presents the numerical values of mean and standard deviation for healthy and BRB conditions during startup transient and steady state, which for each frequency tested (50, 65 and 100 Hz), are used to obtain the first random values applied to K-means algorithm to obtain the initial centroids. Tables II and III present the obtained classification results for startup transient and steady state, respectively. It can be observed that the K-means algorithm classifies, in all cases, healthy condition either in startup transient or steady state, which represents a 100 % of effectiveness, and in the case of BRB in both regimes, the system classifies in 37 of 38 tests, which represents a 97.3% of effectiveness.

TABLE I. MEAN AND STANDARD DEVIATION OF IM

Condition	Frequency (Hz)	Startup transient		Steady state	
		μ	σ	μ	σ
Healthy	50	0.6862	0.0321	0.9426	0.0498
BRB		2.71293	0.6974	3.7457	0.7792
Healthy	65	0.6762	0.02869	0.9522	0.0501
BRB		2.2533	0.7124	3.2352	0.5623
Healthy	100	0.7015	0.0474	0.8956	0.0554
BRB		1.5633	0.6523	2.4562	0.6568

TABLE II. CLASSIFICATION RESULTS FOR STARTUP TRANSIENT TESTS (CONFUSION MATRIX)

Condition	Frequency (Hz)	HLT	1BRB	Effectiveness (%)
HLT	50	**38**	0	100
BRB		1	**37**	97.3
HLT	65	**38**	0	100
BRB		2	**36**	94.7
HLT	100	**32**	6	84.2
BRB		7	**31**	81.5

TABLE III. CLASSIFICATION RESULTS FOR STEADY STATE TESTS
(CONFUSION MATRIX)

Condition	Frequency (Hz)	HLT	1BRB	Effectiveness (%)
HLT	50	**38**	0	100
BRB		1	**37**	97.3
HLT	65	**38**	0	100
BRB		2	**36**	94.7
HLT	100	**38**	0	100
BRB		2	**36**	94.7

A. Discussion

In the present study, the difference when the synthetic signals and stator current signals are analyzed using the proposed RSTFT methodology, and the classical STFT, that it can be observed from time–frequency spectra obtained in Fig. 4 and Fig. 5. Finally, better results are obtained using the proposed methodology for synthetic signals, because the fault related harmonics can be clearly detected during startup transient and steady state as it is shown in Fig. 4. Instead, for stator current signals, the proposed methodology also shows better results than the classical STFT technique, because in the three cases of 50, 65, and 100 Hz, as is shown in Fig. 5. The fault related harmonics (LSH and USH) can be also clearly observed in startup transient and steady state regimes, with the exception of the 100 Hz case, where it is noticed from second 10 to second 12 from the final stage of startup transient, due to a low slip value of the IM during this stage. The low separation of fault related harmonics according to (12); in comparison with the classical STFT that can detect these harmonics related to the 1 BRB fault during steady state. However, during startup transient there is no a clear observation of the LSH and USH because there is a conflict to get a good time resolution or good frequency resolution, but not both when a certain size of window is chosen.

Thus, although in the time-frequency spectra obtained, the fault is clearly detectable and observable, through the use of the proposed classifier. The motor condition can be determined with a high degree of effectiveness, regardless of the frequency of operation as shown in tables II and III. It can be observed that k–means algorithm classifies, for all cases, of healthy condition during startup transient and steady state, almost all the cases (37 of 38) for faulty condition during both regimes at 50 Hz, which represent a good classification effectiveness. Moreover, the proposal methodology gives a) a good visual detectability with a good time and frequency resolution of the fault in startup transient and steady state, and b) an automatic IM condition without the necessity of a large data set of the stator current acquired in the motor.

V. CONCLUSIONS

In this paper, the analysis of current signal for identifying the time evolution of faults for BRB of a VSD-fed IM during the startup transient and steady state is used and analyzed by using the RSTFT, and K-means clustering algorithm for automatic diagnostic of the condition of IM is carried out.

The analysis is contrasted with STFT for synthetic and real signals. The results show that RSTFT has a better resolution, which leads to identify the fault related

harmonics evolution for BRB in both regimes with high accuracy in comparison with STFT. The RSTFT can detect the fault related frequencies, even in the startup transient of the IM VSD fed. Moreover, for automatic diagnosis of fault or healthy conditions of IM, the simple K-means algorithm shows excellent results to classify between the healthy and the fault condition.

Detection of components, related to fault, is an important advantage compared with other techniques that cannot detect the fault related harmonics during startup transient due to low values of motor slip, making these harmonics evolve closely to the fundamental frequency. Moreover, driver induces harmonics that make difficult the detection. Experimental results showed that the proposed method obtained clear features, which could be used to detect, automatically, two different conditions of an induction motor.

For future research, it would be desirable to continue working where low levels of motor slip has to be considered because it is more difficult to detect the fault related harmonics, also, it is important uses different load levels and different types of drivers, which will affect the current signal in a different way by the harmonics that each type of control introduces to the signal.

REFERENCES

[1] V. Ghorbanian and J. Faiz, "A survey on time and frequency characteristics of induction motors with broken rotor bars in line-start and inverter-fed modes", Mechanical Systems and Signal Processing, vol. 54-55, pp. 427-456, 2015. doi:10.1016/j.ymssp.2014.08.022
[2] K. Kim and A.G. Parlos, "Induction Motor Fault Diagnosis Based on Neuropredictors and Wavelet Signal Processing," IEEE/ASME Trans. Mechatronics, vol. 7, no. 2 pp. 201–219, 2002. doi:10.1109/TMECH.2002.1011258
[3] F. Filippetti, G. Franceschini, C. Tassoni and P. Vas, "Recent developments of induction motor drives fault diagnosis using AI techniques," IEEE Transactions on Industrial Electronics, vol.47, pp. 1966-1973, 2000. doi:10.1109/41.873207
[4] M. El Hachemi Benbouzid, "A review of induction motors signature analysis as a medium for faults detection", IEEE Transactions on Industrial Electronics, vol. 47, no. 5, pp. 984-993, 2000. doi:10.1109/41.873206
[5] J. Milimonfared, H.M.Kelk,S.Nandi,A.D.Minassians, and H. A. Toliyat, "A novel approach for broken-rotor-bar detection in cage induction motors," IEEE Trans. Ind. Appl., vol. 35, no. 5, pp.1000–1006, 1999. doi:10.1109/28.793359
[6] J. de Jesus Rangel-Magdaleno, H. Peregrina-Barreto, J. Ramirez-Cortes, P. Gomez-Gil and R. Morales-Caporal, "FPGA-Based Broken Bars Detection on Induction Motors Under Different Load Using Motor Current Signature Analysis and Mathematical Morphology", IEEE Transactions on Instrumentation and Measurement, vol. 63, no. 5, pp. 1032-1040, 2014. doi:10.1109/TIM.2013.2286931
[7] A. Garcia-Perez, R. Romero-Troncoso, E. Cabal-Yepez and R. Osornio-Rios, "The Application of High-Resolution Spectral Analysis for Identifying Multiple Combined Faults in Induction Motors", IEEE Transactions on Industrial Electronics, vol. 58, no. 5, pp. 2002-2010, 2011. doi:10.1109/TIE.2010.2051398
[8] A. Bellini, A. Yazidi, F. Filippetti, C. Rossi and G. Capolino, "High Frequency Resolution Techniques for Rotor Fault Detection of

Induction Machines", IEEE Transactions on Industrial Electronics, vol. 55, no. 12, pp. 4200-4209, 2008. doi:10.1109/TIE.2008.2007004

[9] J. Antonino-Daviu, S. Aviyente, E. G. Strangas, M. Riera-Guasp, J. Roger-Folch, and R.B. Pérez, "An EMD-based invariant feature extraction algorithm for rotor bar condition monitoring", in Proc. IEEE 2011 International Symposium on Diagnostics for Electric Machines, Power Electronics & Drives (SDEMPED), Bologna, Italy, Sept. 2011, pp. 669-675. doi:10.1109/DEMPED.2011.6063696

[10] R. Valles-Novo, J. de Jesus Rangel-Magdaleno, J. Ramirez-Cortes, H. Peregrina-Barreto and R. Morales-Caporal, "Empirical Mode Decomposition Analysis for Broken-Bar Detection on Squirrel Cage Induction Motors", IEEE Transactions on Instrumentation and Measurement, vol. 64, no. 5, pp. 1118-1128, 2015. doi:10.1109/TIM.2014.2373513

[11] R. Romero-Troncoso, D. Moringo-Sotelo, O. Duque-Perez, R. Osornio-Rios, M. Ibarra-Manzano and A. Garcia-Perez, "Broken rotor bar detection in VSD-fed induction motors at startup by high-resolution spectral analysis", in Proc. 2014 International Conference on Electrical Machines (ICEM), Berlin Sept. 2014, pp. 1848-1854. doi:10.1109/ICELMACH.2014.6960435

[12] A. Garcia-Ramirez, R. Osornio-Rios, D. Granados-Lieberman, A. Garcia-Perez and R. Romero-Troncoso, "Smart Sensor for Online Detection of Multiple-Combined Faults in VSD-Fed Induction Motors", Sensors, vol. 12, no. 9, pp. 11989-12005, 2012. doi:10.3390/s120911989

[13] R. Romero-Troncoso, D. Moringo-Sotelo, O. Duque-Perez, P. Gardel-Sotomayor, R. Osornio-Rios and A. Garcia-Perez "Early broken rotor bar detection techniques in VSD-fed induction motors at steady-state", in Proc. IEEE 2013 International Symposium on Diagnostics for Electric Machines, Power Electronics & Drives (SDEMPED), Valencia, Spain, August 2013, pp. 105-113. doi:10.1109/DEMPED.2013.6645704

[14] M. Dlamini, P. Barendse and A. Khan, "Detecting faults in inverter-fed induction motors during startup transient conditions", in Proc. IEEE 2014 Energy Conversion Congress and Exposition (ECCE), Pittsburg, Sept. 2014, pp. 3131-3138. doi:10.1109/ECCE.2014.6953826

[15] J. Pons-Llinares, D. Moringo-Sotelo, O. Duque-Perez, J. Antonino-Daviu and M. Perez-Alonso, "Transient detection of close components through the chirplet transform: Rotor faults in inverter-fed induction motors", in Proc. IECON 2014 - 40th Annual Conference of the IEEE Industrial Electronics Society, Dallas, October 2014, pp. 3386-3392. doi:10.1109/IECON.2014.7048999

[16] J. Pons-Llinares, J. Antonino-Daviu, J. Roger-Folch, D. Moríñigo-Sotelo and O. Duque-Pérez, "Mixed eccentricity diagnosis in Inverter-Fed Induction Motors via the Adaptive Slope Transform of transient stator currents", Mechanical Systems and Signal Processing, vol. 48, no. 1-2, pp. 423-435, 2014. doi:10.1016/j.ymssp.2014.02.012

[17] E. Cabal-Yepez, A. Fernandez-Jaramillo, A. Garcia-Perez, R. Romero-Troncoso and J. Lozano-Garcia, "Real-time condition monitoring on VSD-fed induction motors through statistical analysis and synchronous speed observation". International Transactions on Electrical Energy Systems, 2014. doi:10.1002/etep.1938

[18] J. Faiz, V. Ghorbanian and B. Ebrahimi, "EMD-Based Analysis of Industrial Induction Motors with Broken Rotor Bars for Identification of Operating Point at Different Supply Modes", IEEE Transactions on Industrial Informatics, vol. 10, no. 2, pp. 957-966, 2014. doi:10.1109/TII.2013.2289941

[19] A. Papandreou-Suppappola, "Applications in time-frequency signal processing", vol. 10. pp. 179-203 CRC press, 2002. doi:10.1201/9781420042467

[20] Chassande-Motin, Éric, François Auger, and Patrick Flandrin. "Reassignment." In Time-Frequency Analysis: Concepts and Methods. Edited by Franz Hlawatsch and François Auger. pp. 249-277, London: ISTE/John Wiley and Sons, 2008. doi:10.1002/9780470611203.ch9

[21] B. Akin, U. Orguner, H.A. Toliyat and M. Rayner, "Low order PWM inverter harmonics contributions to the inverter-fed induction machine fault diagnosis," IEEE Transactions on Industrial Electronics, vol. 55, no. 2, pp. 610–619, 2008. doi:10.1109/TIE.2007.911954

[22] B. Ayhan, H. Joel Trusell, M.-Y. Chow, and M.-H. Song, "On the use of a lower sampling rate for broken rotor bar detection width DTFT and AR-based spectrum methods," IEEE Transactions on Industrial Electronics, vol. 55, no. 3, pp. 1421–1434, Mar. 2008. doi:10.1109/TIE.2007.896522

[23] S. Pan, T. Han, A. C. C. Tan, and T. R. Lin, "Fault diagnosis system of induction motors based on multiscale entropy and support vector machine with mutual information algorithm," Shock and Vibration, vol. 2016, Article ID 5836 717, 12 pages, 2016. doi:10.1155/2016/5836717

[24] A. Guerra de Araujo Cruz, R. Delgado Gomes, F. Antonio Belo and A. Cavalcante Lima Filho, "A Hybrid System Based on Fuzzy Logic to Failure Diagnosis in Induction Motors", IEEE Latin America Transactions, vol. 15, no. 8, pp. 1480-1489, 2017. doi:10.1109/TLA.2017.7994796

[25] J. Amezquita-Sanchez, M. Valtierra-Rodriguez, C. Perez-Ramirez, D. Camarena-Martinez, A. Garcia-Perez and R. Romero-Troncoso, "Fractal dimension and fuzzy logic systems for broken rotor bar detection in induction motors at start-up and steady-state regimes", Measurement Science and Technology, vol. 28, no. 7, p. 075001, 2017. doi:10.1088/1361-6501/aa6adf

[26] L. Maraaba, Z. Al-Hamouz and M. Abido, "An Efficient Stator Inter-Turn Fault Diagnosis Tool for Induction Motors", energies, vol.11, no.3, March 2018. doi:10.3390/en11030653

[27] F. Khater, M. Abu El-Sebah and M. Osama, "Fault diagnostics in an inverter feeding an induction motor using fuzzy logic", Journal of Electrical Systems and Information Technology, vol. 4, no. 1, pp. 10-17, 2017. doi:10.1016/j.jesit.2016.10.005

[28] L. Maraaba, Z. Al-Hamouz and M. Abido, "An Efficient Stator Inter-Turn Fault Diagnosis Tool for Induction Motors", Energies, vol. 11, no. 3, p. 653, 2018. doi: 10.3390/en11030653

[29] A. Glowacz, "Acoustic based fault diagnosis of three-phase induction motor", Applied Acoustics, vol. 137, pp. 82-89, 2018. doi:10.1016/j.apacoust.2018.03.010

[30] D. Chen andW. J.Wang, "Classification of wavelet map patterns using multi-layer neural networks for gear fault detection," Mechanical Systems and Signal Processing, vol. 16,no. 4, pp. 695– 704, 2002. doi:10.1006/mssp.2002.1488

[31] V. N. Ghate and S. V. Dudul, "Optimal MLP neural network classifier for fault detection of three phase induction motor," Expert Systems with Applications, vol. 37, no. 4, pp. 3468–3481, 2010. doi:10.1016/j.eswa.2009.10.041

[32] Z. Liu, H. Cao, X. Chen, Z. He and Z. Shen, "Multi-fault classification based on wavelet SVM with PSO algorithm to analyze vibration signals from rolling element bearings", Neurocomputing, vol. 99, pp. 399-410, 2013. doi:10.1016/j.neucom.2012.07.019

[33] P. Chauhan and M. Shukla, "A review on outlier detection techniques on data stream by using different approaches of K-means algorithm", in Proc. International Conference on Advances in Computer Engineering and Applications (ICACEA), Ghaziabad, India, March 2015, pp. 580 – 585.doi:10.1109/ICACEA.2015.7164758

[34] D. Camarena-Martinez, M. Valtierra-Rodriguez, J. Amezquita-Sanchez, D. Granados-Lieberman, R. Romero-Troncoso and A. Garcia-Perez, "Shannon Entropy and K-means Method for Automatic Diagnosis of Broken Rotor Bars in Induction Motors Using Vibration Signals". Shock and vibrations, 2016. doi:10.1155/2016/4860309

[35] C.T.Yiakopoulos, K. C. Gryllias, and I. A. Antoniadis, "Rolling element bearing fault detection in industrial environments based on a K-means clustering approach", Expert Systems with Applications, vol. 38, no. 3, pp. 2888–2911, 2011. doi: 10.1016/j.eswa.2010.08.083